PHYSICAL REVIEW B **90**, 241416(R) (2014)

Photon-drag-induced terahertz emission from graphene

Petr A. Obraztsov,[1,2,*] Natsuki Kanda,[3,4] Kuniaki Konishi,[5] Makoto Kuwata-Gonokami,[4,5,6] Sergey V. Garnov,[1] Alexander N. Obraztsov,[2,7] and Yuri P. Svirko[2]

[1]*A. M. Prokhorov General Physics Institute, Moscow, Russia*
[2]*Department of Physics and Mathematics, University of Eastern Finland, Joensuu, Finland*
[3]*Laser Technology Laboratory, RIKEN, Saitama, Japan*
[4]*Photon Science Center, The University of Tokyo, Tokyo, Japan*
[5]*Institute for Photon Science and Technology, The University of Tokyo, Tokyo, Japan*
[6]*Department of Physics, The University of Tokyo, Tokyo, Japan*
[7]*Department of Physics, M. V. Lomonosov Moscow State University, Moscow, Russia*

(Received 9 October 2014; published 29 December 2014)

We report the investigation of a strong interband photon drag effect in multilayer graphene leading to efficient emission of terahertz radiation. The obtained terahertz photoresponse of graphene layers exhibits peculiarities fundamentally predicted for free carrier transport in two-dimensional electronic systems. Owing to significant light absorption in gapless graphene, where each absorbed photon produces an electron-hole pair with the highest possible kinetic energy, the photon drag mechanism provides a possibility to achieve efficient conversion of light into broadband terahertz radiation as well as new ways towards vectorial control of the generated terahertz radiation in graphene-based materials.

DOI: 10.1103/PhysRevB.90.241416 PACS number(s): 78.67.Wj, 42.65.Re, 78.66.Hf

Nanocarbon materials—those with dominating sp^2 hybridization of orbitals and especially graphene—have recently attracted great attention because of their ability to support ballistic electron transport [1,2]. The submicron free pass, ultrafast energy relaxation, and relatively low momentum relaxation rates make these materials interesting for optoelectronics [3], spintronics [4], valleytronics [5], and quantum computing [6]. It is worth noting that in gapless graphene, the whole absorbed photon energy $\hbar\omega$ is transformed into the kinetic energy of photoexcited carriers. Correspondingly, one may expect that the role of the kinetic effects should be pronounced in the linear and nonlinear optical response because the generated electron-hole pairs possess the highest possible kinetic energy. However, despite the anomalous electron mobility and the ballistic current-carrying capability, studies on the injection and control of ballistic currents in graphene and other nanocarbon materials with sp^2 orbital hybridization are scarce [7–13].

We have previously demonstrated that combinations of quasiballistic conductivity and strong electron-phonon coupling in graphene-based materials opens an opportunity to launch transient photocurrents in a prescribed direction by transferring the photon momentum to electrons [14–17]. This phenomenon is referred to as the photon drag effect and manifests itself as a direct current (dc) generated under illumination by an intense light beam [18–21]. In nanowires made of carbon nanotubes [15] and nanographite films [14,16,17], the considerable photon drag effect gives rise to strong dc current under irradiation with nanosecond laser pulses in the visible to near-IR range. The direction and magnitude of the current induced by the laser pulse in nanographite films can be manipulated by the incidence angle and polarization of the laser beam. Also, dragging carriers by low-energy photons due to intraband absorption in single-layer graphene has been theoretically discussed in [22,23] and experimentally observed in [24]. However, the latter experiments were mainly focused on the photon helicity dependent photogalvanic currents occurring under intraband excitation (in far-IR or terahertz range) of micron-sized graphene flakes where electron kinetics was strongly influenced by the boundaries of employed samples and electrodes attached to the graphene surface. In addition, the time-integrated techniques employed to measure graphene photocurrent response were hindering the real origin of the induced polarization-dependent charge currents. Here we report on observation of efficient terahertz emission from unbiased multilayer graphene (MG) excited with femtosecond laser pulses centered at 800 nm. Taking advantage of contactless terahertz emission spectroscopy we demonstrate that the terahertz signal originates from quasiballistic lateral photon drag currents occurring in graphene under interband transitions.

The multilayer graphene samples employed in our experiments were grown using a plasma-assisted chemical vapor deposition technique on Ni substrates [25]. The obtained MG samples were wet etched and then transferred onto the SiO_2 substrates. Different samples with numbers of layers ranging from 1 to approximately 30 were studied in the experiments. The number of graphene layers in the MG samples and the high crystalline quality in the MG samples were confirmed with optical transmission [26] and Raman spectroscopy methods [27].

In order to investigate the subpicosecond photocurrent induced by femtosecond light pulses in the MG samples, we performed time-resolved measurements of produced electric fields (terahertz pulses). In the experiment, the output beam of a Ti:sapphire laser (Coherent RegA 9000: 800 nm; 200 fs; 120 kHz) was split into two parts: an intense pump beam and a weak reference beam. In all experiments, the pump beam was linearly polarized and the angle between the electric field vector E and the incidence plane was controlled with a half-wave plate coupled with a polarizer. The incidence angle of the pump beam was always set to $\alpha = 45^\circ$ and the beam

*p.obraztsov@gmail.com

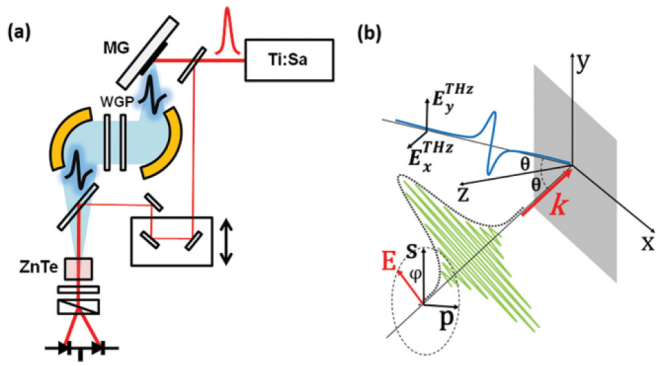

FIG. 1. (Color online) (a) Experimental setup for terahertz emission measurements. (b) Schematic of the terahertz emission experiment in reflection configuration.

diameter on the sample surface was less than 5 mm. The optical scheme of the experimental setup is shown in Fig. 1. The induced terahertz emission from the sample was collected in a reflection configuration with a gold parabolic mirror and then focused on a ZnTe electro-optic crystal together with the delayed reference beam. In order to determine both the magnitude and polarization of the emitted terahertz wave, each measurement was performed twice: with and without the 45° wire-grid polarizer inserted between the sample and the parabolic mirror (see Fig. 1). We employed the electro-optic detection system consisting of a wave plate, a Wollaston prism, two balanced photodiodes connected to a lock-in amplifier, and a Fourier transform to reveal the magnitude and phase of the generated terahertz signals.

The maximum magnitude of the terahertz field obtained from the MG samples was about four times less than that generated in the reference GaAs at the same pump intensity. The time-domain waveform, spectrum, and dependence of the terahertz signal on the pump power are presented in Figs. 2(a) and 2(b). The observed linear dependence of the terahertz field on the light intensity shown in the inset of Fig. 2(b) is indicative of a second-order nonlinear process. It is worth noting that we did not observe any changes in the terahertz field when the sample was rotated around the substrate normal. This indicates that the normal of the studied MG samples coincides with a sixfold rather than a threefold rotation axis [28].

Our measurements showed that the magnitude of the generated terahertz field decreases with an increase in the number of graphene layers. This can be explained by a higher number of defects in thicker samples that results in suppression of the light-induced lateral currents generated in the topmost graphene layers. Also, increasing the number of stacked graphene layers in the MG samples decreases the electron-phonon coupling which, in terms of photon drag, leads to less efficient terahertz emission from the thicker samples.

The amplitudes of the E_x- and E_y-polarized components of the terahertz field generated in all the samples shows $\cos 2\phi$- and $\sin 2\phi$-like dependence, respectively, on the pump polarization azimuth φ [see Fig. 1(b)]. This experimental finding confirms that the mechanism of the terahertz emission in MG is different from that in bulk graphite. It has been recently suggested [29] that in highly oriented pyrolitic graphite (HOPG) irradiated with femtosecond light pulses, terahertz radiation is generated by a transient photocurrent in a direction normal to the graphene planes, i.e., along the c axis of the graphite crystal. This resembles the terahertz generation in strongly absorbing semiconductors in which different diffusion constants of electrons and holes leads to the buildup of a space-charge field (the photo-Dember effect) [30]. In such a case, the time-dependent dipole that emits the terahertz field is oriented perpendicular to the photoexcited surface. The terahertz radiation is coupled out very efficiently when the surface is excited under 45° and the terahertz radiation is detected in the direction of specular reflection. Similarly, the difference of the electron and hole mobility along the HOPG c axis can give rise to the time-dependent dipole, which is oriented along the surface normal and emits terahertz radiation. However in our experiment, the polarization of the emitted terahertz field, and thus the orientation of the dipole, depends on the polarization of the excitation beam. This indicates that the femtosecond light pulses produce coherent transient lateral currents depending on the polarization of the excitation beam, angle of incidence, and symmetry of the sample.

The constitutive equation that describes the induced in-plane photocurrent density can be presented in the following form:

$$J_i = \chi_{ijk} E_j E_k^* + \frac{i}{2} T_{ijkl}\{E_j(\nabla_l E_k^*) - (\nabla_l E_j)E_k^*\}, \qquad (1)$$

where the subscripts indicate Cartesian coordinates in the laboratory frame with the z axis along the graphene normal and $\boldsymbol{E}$ is the complex amplitude of the electric field in the light wave. The material tensor χ_{ijk} describes the linear photogalvanic effect (LPGE) [31], which may contribute to the current density because placing the MG onto a dielectric

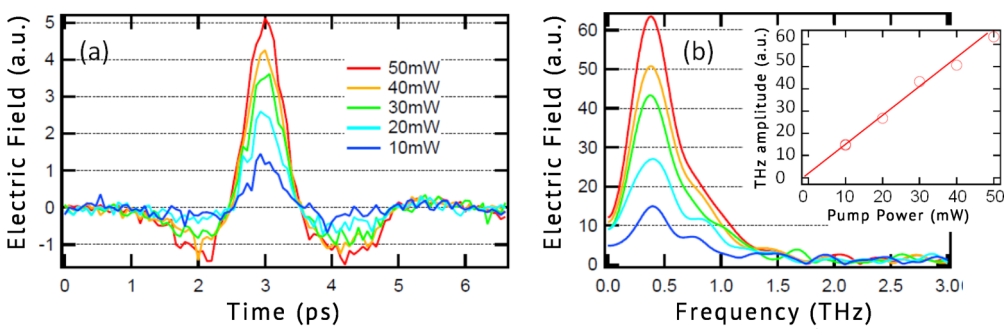

FIG. 2. (Color online) Terahertz emission from an MG sample: (a) time-domain waveforms and (b) Fourier transformed spectra measured at different excitation powers. The pump power dependence is shown in the inset of (b).

substrate can result in lifting the inversion symmetry of the MG. The material tensor T_{ijkl} describes the current originating from the linear photon drag [20] and quadrupole optical rectification [32] effects. By taking into account that the sixfold symmetry axis along the graphene normal $\boldsymbol{n}$ reduces the number of independent components of $\chi_{ijk} = \chi_{ikj}$ and $T_{ijkl} = T_{ikjl}$ down to four and six, respectively, Eq. (1) for the Cartesian components of the in-plane terahertz current density induced by a linearly polarized beam in graphene yields

$$J_{x,y} = 2\chi_{xxz}E_z^* E_{x,y} + T_{xyyx}(|E_x|^2 + |E_y|^2)k_{x,y} + 2T_{xxyy}(k_x E_x^* + k_y E_y^*)E_{x,y} + T_{xzzx}|E_z|^2 k_{x,y}. \quad (2)$$

The constitutive equation (2) allows us to obtain the orthogonal components E_x and E_y of the terahertz field $\boldsymbol{E}^{\mathrm{THz}} \propto \partial \boldsymbol{J}/\partial t$ radiated by graphene in the specular direction [see Fig. 1(b)]:

$$E_Y^{\mathrm{THz}} \propto \left[\chi_{xxz} + \frac{\omega n}{c} T_{xxyy}\cos\theta_1\right] t_s t_p \sin 4\phi \sin\theta,$$

$$E_X^{\mathrm{THz}} \propto \left[\chi_{xxz}\sin^2 2\phi \cos\theta_1 + \frac{\omega n}{c} \times \left\{\left[\left(T_{xxyy} + \frac{T_{xyyx}}{2}\right)\cos^2\theta_1 + \frac{T_{xzzx}}{n^2}\sin^2\theta\right] \times \sin^2 2\phi + \frac{T_{xyyx}}{2}\frac{t_s^2}{t_p^2}\cos^2 2\phi\right\}\right] t_p^2 \sin\theta, \quad (3)$$

where n is the refractive index of the substrate, ϕ is the angle defining the position of the half-wave plate axis, t_s and t_p are transmission coefficients of the substrate-vacuum interface in the presence of the MG for the s-polarized ($\phi = 0$) and p-polarized ($\phi = \pi/4$) excitation beams, respectively, and $\cos\theta_1 = \sqrt{1 - (\sin\theta/n)^2}$. The first and second terms in square brackets in Eqs. (3) describe the current density originating from the linear photogalvanic and photon drag effects, respectively. One can observe from Eqs. (3) that the terahertz field strongly depends on both the polarization and angle of incidence of the excitation beam and that the photon drag and linear photogalvanic effects give additive contributions to the signal.

Among alternatives to the photon drag mechanisms of the lateral photocurrents in MG samples, we consider the surface photogalvanic effect (SPGE) [33] that originates from the influence of the interface on the light-induced electron kinetics. Specifically, in close vicinity of the surface, electrons moving towards the bulk of the film will conserve their momentum for a longer time than electrons moving towards the surface. As a result, the momentum distribution of electrons in the subsurface layer becomes anisotropic giving rise to the surface electron current observed in a number of semiconductors. The SPGE can be presented in the following constitutive equation: $J_i^{\mathrm{SPGE}} = \chi_{mjkl}^S (\delta_{im} - n_m n_i) E_j E_k^* n_l$, where n is a unique vector along the surface normal that coincides with the z axis of the Cartesian laboratory frame. One can observe that the surface current changes polarity when the sign of n is reversed, i.e., currents associated with the vacuum-graphene and graphene-substrate interfaces will compensate one another. Thus, in an ideal graphene one may expect a total cancellation of the terahertz emission originating from the SPGE. However, in a MG sample of a finite thickness, the cancellation of the surface currents will be incomplete because the light intensity at the bottom surface will be less than that at the front surface because of light absorption in the sample. The SPGE contribution to the light-induced photoresponse on nanosecond time scales has been recently observed in films composed of micron-sized graphene flakes [16]. However, in the MG samples the SPGE should vanish for an s-polarized excitation beam ($\phi = \pi/2$; see Fig. 3), while in our experiments we observed terahertz signals of comparable magnitudes for both s- and p-polarized excitation. This allows us to conclude that the SPGE does not contribute to the observed effect.

In practice, separation of these contributions requires additional measurements, e.g., a study of the dependence of the terahertz field amplitude excitation wavelength. In our experiment, we made use of the fact that the photon drag current is an odd function of the wave vector, i.e., it changes sign when $\boldsymbol{k}$ is replaced with $-\boldsymbol{k}$, while the photogalvanic

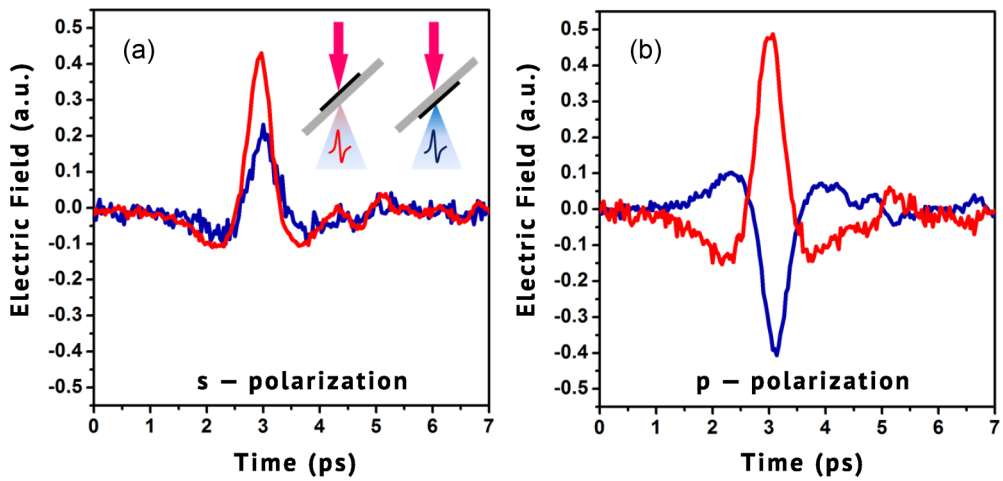

FIG. 3. (Color online) Terahertz emission time-domain waveforms obtained from an MG sample in the transmission configuration. Red lines and blue lines correspond to excitation from graphene and substrate sides, respectively. (a) Excitation with an s-polarized laser beam. (b) Excitation with a p-polarized beam.

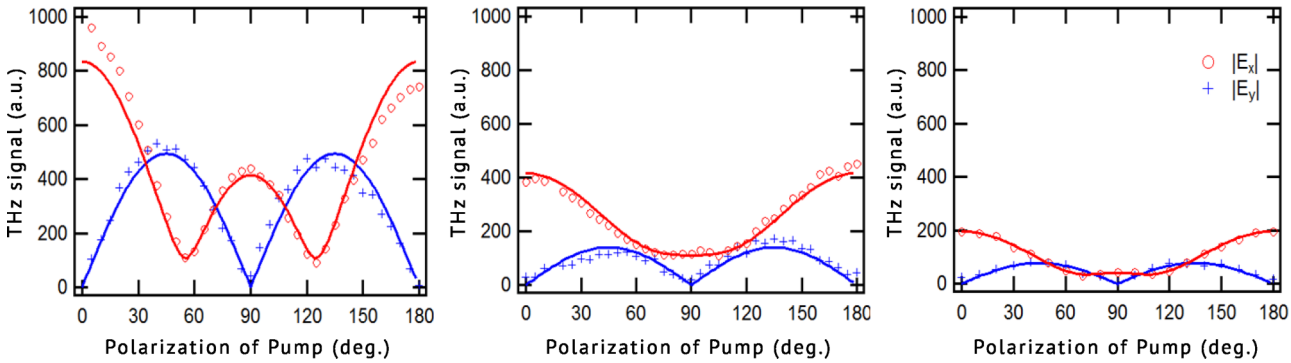

FIG. 4. (Color online) Absolute values of the x (red circles) and y components (blue crosses) of the terahertz field generated in three MG samples with different numbers of graphene layers as a function of the polarization plane azimuth. The number of layers increases from left to right. Solid lines correspond to the fitting with Eq. (3).

current does not. Thus, by comparing the sign of the terahertz waveform generated in the sample when the direction of the excitation beam is reversed, one can visualize the mechanism that dominates the terahertz emission.

In order to detect the direction of the terahertz current generated in graphene due to photon drag and/or the photogalvanic effect, we performed independent measurements with the 15-nm-thick graphene sample in transmittance geometry. The dielectric SiO_2 substrate was thin enough to allow us to perform measurements in transmission configuration (see Fig. 3). We observe that when the sample is irradiated with a p-polarized beam from the substrate side, the polarity of the generated terahertz waveform changes to the opposite, while excitation with an s-polarized beam does not result in a change of the signal polarity, i.e., a π phase shift occurs. The magnitudes of the signals obtained when the sample was irradiated from the graphene and substrate sides were slightly different because of substrate losses (see Fig. 3). This experimental finding clearly indicates that the photon drag effect dominates the in-plane terahertz current generated in graphene at 800-nm excitation.

Therefore, in Eq. (3) one can neglect the first term in square brackets that describes the photogalvanic effect:

$$E_X^{\mathrm{THz}} \propto T_{xxyy} t_s t_p \cos\theta_1 \sin 4\phi \sin\theta,$$

$$E_Y^{\mathrm{THz}} \propto \left[\left(T_{xxyy} + \frac{T_{xyyx}}{2}\right) t_p^2 \cos^2\theta_1 \sin^2 2\phi + \frac{T_{xyyx}}{2} t_s^2 \cos^2 2\phi\right] \times \sin\theta. \quad (4)$$

In Eq. (4) we have also taken into account that for interband transitions, in-plane carrier motions dominate electronic properties of graphene [10] and hence $|T_{xzzx}| \ll |T_{xyyx}|$. One can observe from Fig. 4 that the equation fully describes the magnitude and polarization dependence of the terahertz field generated in graphene.

In conclusion, polarization-sensitive measurements of the terahertz emission from multilayered graphene films excited with femotescond laser pulses demonstrate that terahertz emission originates from the photon drag effect. The pronounced dependence of the effect on the polarization of the pump optical pulse in graphene-based materials demonstrates that direct transfer of momentum of the electromagnetic radiation to free carriers can be employed for coherent control of the light-induced carrier motion in these materials.

Note added. Recently we became aware of other papers of relevance [34,35].

We would like to thank Y. Okane for performing the measurements, and T. Higuchi, N. Nemoto, and H. Tamaru for a fruitful discussion. The research was partially supported by the Russian Foundation for Basic Research (Grant No. 12-02-01369) and the President of the Russian Federation Program for Support of Young Scientists (Grant No. MK-2143.2013.2), Russian Science Foundation (Grant No. 14-12-00511), the Photon Frontier Network Program, KAKENHI (20104002), Project for Developing Innovation Systems of the Ministry of Education, Culture, Sports, Science and Technology, Japan, and by JSPS through its FIRST Program.

[1] P. Avouris, Z. Chen, and V. Perebeinos, Nat. Nanotechnol. **2**, 605 (2007).
[2] A. K. Geim and K. S. Novoselov, Nat. Mater. **6**, 183 (2007).
[3] F. Bonaccorso, Z. Sun, T. Hasan, and A. C. Ferrari, Nat. Photonics **4**, 611 (2010).
[4] D. A. Pesin and A. H. MacDonald, Nat. Mater. **11**, 409 (2012).
[5] Y. Jiang, T. Low, K. Chang, M. I. Katsnelson, and F. Guinea, Phys. Rev. Lett. **110**, 046601 (2013).
[6] A. Rycerz, J. Tworzydlo, and C. W. J. Beenakker, Nat. Phys. **3**, 172 (2007).
[7] D. Sun, C. Divin, J. Rioux, J. E. Sipe, C. Berger, W. A. de Heer, P. N. First, and T. B. Norris, Nano Lett. **10**, 1293 (2010).
[8] J. Rioux, G. Burkard, and J. E. Sipe, Phys. Rev. B **83**, 195406 (2011).
[9] D. Sun, G. Aivazin, A. M. Jones, J. S. Ross, W. Yao, D. Codben, and X. Xu, Nat. Nanotechnol. **7**, 114 (2012).

[10] L. Prechtel, L. Song, D. Schuh, P. Ajayan, W. Wegscheider, and A. W. Holleitner, Nat. Commun. **3**, 646 (2012).
[11] D. Sun, J. Rioux, J. E. Sipe, Y. Zou, M. T. Mihnev, C. Berger, W. A. de Heer, P. N. First, and T. B. Norris, Phys. Rev. B **85**, 165427 (2012).
[12] E. Hendry, P. J. Hale, J. J. Moger, A. K. Savchenko, and S. A. Mikhailov, Phys. Rev. Lett. **105**, 097401 (2010).
[13] E. J. Mele, P. Král, and D. Tománek, Phys. Rev. B **61**, 7669 (2000).
[14] G. M. Mikheev, R. G. Zonov, A. N. Obraztsov, and Y. P. Svirko, Appl. Phys. Lett. **84**, 4854 (2004).
[15] A. N. Obraztsov, D. A. Lyashenko, S. Fang, R. H. Baughman, S. V. Garnov, and Y. P. Svirko, Appl. Phys. Lett. **94**, 231112 (2009).
[16] P. A. Obraztsov, G. M. Mikheev, S. V. Garnov, A. N. Obraztsov, and Y. P. Svirko, Appl. Phys. Lett. **98**, 091903 (2011).
[17] P. A. Obraztsov, T. Kaplas, S. V. Garnov, M. K. Gonokami, A. N. Obraztsov, and Y. P. Svirko, Sci. Rep. **4**, 4007 (2014).
[18] A. M. Danishevskii, A. A. Kastal'skii, S. M. Ryvkin, and I. D. Yaroshetskii, Sov. Phys. JETP **31**, 292 (1970).
[19] I. I. Boiko, Phys. Status Solidi B **55**, K149 (1973).
[20] A. A. Grinberg and S. Luryi, Phys. Rev. B **38**, 87 (1988).
[21] R. Loudon, S. M. Barnett, and C. Baxter, Phys. Rev. A **71**, 063802 (2005).
[22] M. V. Entin, L. I. Magarill, and D. L. Shepelyansky, Phys. Rev. B **81**, 165441 (2010).
[23] K. L. Ishikawa, Phys. Rev. B **82**, 201402(R) (2010).
[24] M. M. Glazov and S. D. Ganichev, Phys. Rep. **535**, 101 (2014).
[25] A. N. Obraztsov, E. A. Obraztsova, A. V. Tyurnina, and A. A. Zolotukhin, Carbon **45**, 2017 (2007).
[26] R. R. Nair, P. Blake, A. N. Grigorenko, K. S. Novoselov, T. J. Booth, T. Stauber, N. M. R. Peres, and A. K. Geim, Science **320**, 1308 (2008).
[27] A. C. Ferrari, J. C. Meyer, V. Scardaci, C. Casiraghi, M. Lazzeri, F. Mauri, S. Piscanec, D. Jiang, K. S. Novoselov, S. Roth, and A. K. Geim, Phys. Rev. Lett. **97**, 187401 (2006).
[28] J. E. Sipe and A. I. Shkrebtii, Phys. Rev. B **61**, 5337 (2000).
[29] G. Ramakrishnan, R. Chakkittakandy, and P. C. M. Planken, Opt. Express **17**, 16092 (2009).
[30] G. Klatt, F. Hilser, W. Qiao, M. Beck, R. Gebs, A. Bartels, K. Huska, U. Lemmer, G. Bastian, M. B. Johnston, M. Fischer, J. Faist, and T. Dekorsy, Opt. Express **18**, 4939 (2010).
[31] V. L. Gurevich and R. Laiho, Phys. Rev. B **48**, 8307 (1993).
[32] J. L. W. Siders, S. A. Trugman, F. H. Garzon, R. J. Houlton, and A. J. Taylor, Phys. Rev. B **61**, 13633 (2000).
[33] V. L. Al'perovich, V. I. Belinicher, V. N. Novikov, and A. S. Terekhov, Sov. Phys. JETP **6**, 1201 (1981).
[34] Y.-M. Bahk, G. Ramakrishnan, J. Choi, H. Song, G. Choi, Y. H. Kim, K. J. Ahn, D.-S. Kim, and P. C. M. Planken, ACS Nano **8**, 9089 (2014).
[35] J. Maysonnave, S. Huppert, F. Wang, S. Maero, C. Berger, W. de Heer, T. B. Norris, L. A. De Vaulchier, S. Dhillon, J. Tignon, R. Ferreira, and J. Mangeney, Nano Lett. **14**, 5797 (2014).